Evaluation of the right parasternal four-chamber view for the assessment of left ventricular longitudinal strain and strain rate by two-dimensional speckle tracking echocardiography in dogs

Giorgia Santarelli [a, b] DVM, MSc

Jesús Talavera López [a, b] DVM, PhD

Josefa Fernández del Palacio [a, b] DVM, PhD, Dipl ECVIM-CA (Cardiology)

[a] Division of Veterinary Cardiology-Pulmonology, Veterinary Teaching Hospital, University of Murcia, Campus Espinardo, 30100, Murcia, Spain.

[b] Department of Veterinary Medicine and Surgery, Faculty of Veterinary Medicine, University of Murcia, Campus Espinardo, 30100, Murcia, Spain.

Address correspondence to Dr. Santarelli (Giorgia.Santarelli@ed.ac.uk),

Present address: Cardiopulmonary Service, Hospital for Small Animals, Royal (Dick) School of Veterinary Studies, University of Edinburgh, Easter Bush Campus, EH25 9RG, Roslin, Scotland.

Abstract – Two-dimensional (2-D) speckle tracking echocardiography (STE) is a relatively new imaging technique, introduced in veterinary medicine to aid the assessment of left ventricular (LV) myocardial function. Among other indices, LV longitudinal strain and strain rate (SR) can be measured with this modality, and in dogs they are usually obtained from the left apical four-chamber (LAp4Ch) view. However, in this species, a good quality right parasternal four-chamber (RP4Ch) view can generally be attained, and the aim of this study was therefore to determine its feasibility and reliability for longitudinal strain and SR assessment, and to establish whether the two projections can be used interchangeably. Fifty-one healthy dogs and twenty-five dogs with various cardiac diseases were examined. Longitudinal global and segmental strains and global SR of the LV were obtained with 2-D STE by use of RP4Ch and LAp4Ch views. Intra-observer (within-day and between-day) and inter-observer variabilities were established, and strain and SR values obtained from the two views were compared.

The RP4Ch view demonstrated to be feasible for the assessment of longitudinal strain and SR by use of 2-D STE in healthy and diseased dogs. However, out of sector motion of the apical segments could occur and induce tracking errors. The deformation parameters obtained from this view and the LAp4Ch view were often significantly different, and therefore they should not be used interchangeably. Further, the software employed in the present study performed better global than segmental strain analysis for both views.

Keywords: Canine, Two-dimensional speckle tracking echocardiography, Left ventricular longitudinal strain, Left ventricular longitudinal strain rate, Right parasternal four-chamber view

Conflict of interest

This research did not receive any specific grant from funding agencies in the public, commercial, or not-for-profit sectors.

ABBREVIATIONS

2-D	Two-dimensional
CV	Coefficient of variation
ECG	Electrocardiography
ICC	Intra-class correlation coefficient
LAp4Ch	Left apical four-chamber
LV	Left ventricle
RP4Ch	Right parasternal four-chamber
ROI	Region of interest
SD	Standard deviation
SR	Strain rate
STE	Speckle tracking echocardiography

Introduction

Two-dimensional (2-D) speckle tracking echocardiography (STE) constitutes a relatively new cardiac imaging technique, introduced in veterinary medicine to perform deformation analysis and support noninvasive assessment of left ventricular (LV) myocardial function (Chetboul et al., 2007). Deformation parameters assessed by 2-D STE include the so-called Lagrangian strain, defined as the length of a myocardial segment at end-systole compared to its relaxed length at end-diastole, and strain rate (SR), which represents the change in length per unit of time (Armstrong and Ryan, 2010a; Blessberger and Binder, 2010; Voigt et al., 2015). These deformation indices can be calculated for specific vectors of directions, so that longitudinal, circumferential and radial strains can be obtained, representing different components of contraction (Blessberger and Binder, 2010). To perform strain analysis, 2-D STE uses a post-processing computer algorithm that tracks over time the motion of stable patterns of speckles, a series of artefacts that follow the myocardial movement and are generated at random by reflection, refraction and scattering of ultrasound beams (Armstrong and Ryan, 2010a, 2010b; Blessberger and Binder, 2010; Chetboul et al., 2007; Gorscan III and Tanaka, 2011; Hein et al., 2015; Voigt et al., 2015).

Two-dimensional STE has demonstrated to provide accurate measurements of LV dimensions and strains when validated against sonomicrometry in an experimental study in dogs (Amundsen et al., 2006), and diverse deformation parameters have shown good correlation with invasive indices of LV function, assessed as maximal rate of LV pressure increase (Culwell et al., 2011). Adequate feasibility, reproducibility, and repeatability for its use to aid LV assessment in healthy awake and sedated subjects have been reported (Chetboul et al., 2007, 2008; Santarelli et al., 2017; Wess et al., 2011). Moreover, various 2-D STE derived indices of LV function have been evaluated in canine patients with differing severities of myxomatous mitral valve disease (Smith et al., 2012; Suzuki et al., 2013; Zois et al., 2012, 2013a, 2013b), dilated cardiomyopathy (Chetboul et al., 2007, 2008), and before and after closure of patent ductus arteriosus (Chetboul et al., 2007, 2008; Hamabe et al., 2015; Spalla et al., 2016a, 2016b). Finally, 2-D STE has been used to assess LV function in various canine models of cardiac disease, including Duchenne muscular dystrophy (Takano et al., 2011).

For the evaluation of LV longitudinal strain and SR, the standard left apical four-chamber (LAp4Ch) view is typically used in dogs, as it is in humans and cats (Lang et al., 2015; Silva et al., 2013; Sugimoto et al., 2015). However, a good quality four-chamber image is not always easy to obtain in canine patients from the left parasternal apical location, and in some cases, this view has been associated with tracking errors, especially due to side lobe artifacts that can invalidate strain data from the LV free wall (Griffiths et al., 2011; Wess et al., 2011). In horses, a modified four-chamber view obtained adjusting the standard right parasternal four-chamber (RP4Ch) view is used for analysis of longitudinal strain (Decloedt et al., 2011, 2012). Similarly, the RP4Ch view has been adopted for the purpose in goats, and the analysis demonstrated to be feasible (Berli et al., 2015). The conformation of the canine thorax allows the attainment of good quality right parasternal long–axis images, and the four-chamber view obtained from this approach has been previously compared with that imaged from the left parasternal apical location for the measurement of LV volumes and ejection fraction (Dukes-McEwan, 2002; Wess et al., 2010).

To the authors' knowledge, the use of the RP4Ch view for the assessment of longitudinal strain and SR has not been systematically investigated in dogs. The objective of the study reported here was therefore to determine the feasibility and reliability of the RP4Ch view for longitudinal strain and SR assessment in dogs, and to compare the values obtained from this view and the LAp4Ch view to establish whether the two projections can be used interchangeably.

Materials and Methods

Study population

Healthy and diseased client-owned dogs of any age and weight were prospectively recruited (from January 2015 until July 2018) at the Veterinary Teaching Hospital of the University of Murcia, and they were enrolled during routine consultations or belonged to staff members and students of the University of Murcia. Dogs were eligible for inclusion only if they had a complete electrocardiography (ECG)-gated echocardiography, with excellent-quality images and adequate frame rate (at least 60 Hz) that would allow reliable longitudinal strain analysis. The animals were considered healthy, or affected by a cardiac disease on the basis of the medical history and results of at least a physical examination, complete blood count, blood biochemical analysis, noninvasive blood pressure measurement, ECG, and conventional echocardiography. Additional exams were realized in specific cases if needed, such as thoracic radiography when congestive heart failure was suspected. Diagnosis of cardiac disease was based on commonly used echocardiographic criteria (Boon, 2011), and dogs with any concurrent extra-cardiac disease were excluded. The Owner consent was obtained for each dog before it was enrolled in the study. The study protocol was approved by the Ethics Committee of the University of Murcia.

Echocardiographic examination

The echocardiographic examinations were performed by use of a commercially available ultrasound unit[a] equipped with a multifrequency 1- to 5-MHz phased-array sector transducer with simultaneous ECG recording. The echocardiograms were obtained by a board-certified cardiologist (MJFP) or a supervised cardiology resident (GS) in accordance with published veterinary recommendations (Boon, 2011; Thomas et al., 1993). During examination, the dogs were gently restrained first in right and then in left lateral recumbences. Mild sedation with a combination of acepromazine (0,02 mg/Kg) and butorphanol (0,2 mg/Kg) given intramuscularly was permitted if needed. All data were obtained for at least 4 consecutive cardiac cycles during stable sinus rhythm.

Each echocardiographic examination was stored digitally for offline analysis, and measurements were obtained at a different time point by a single board-certified cardiologist (MJFP), using standard methods described elsewhere (Boon, 2011; Lang et al., 2005, 2015; Quiñones et al., 2002). Mean values over 3 cardiac cycles were used for statistical analysis.

Two-dimensional speckle tracking echocardiography

For analysis of 2-D STE data, images were recorded at rates of 60 to 90 Hz for at least 4 consecutive cardiac cycles**.** The LV strain analysis was performed offline on a separate personal computer by use of dedicated software[b]. Recordings of good quality 2-D cine loops of the LV recorded from the LAp4Ch view and the RP4Ch view were used for assessment of longitudinal strain and SR.

Longitudinal strain was obtained by manual placement of 3 reference points (one on each side of the mitral valve annulus and the third at the apical endocardial border), after choosing the option “AP4”. The software then created a region of interest (ROI) with the automatic delineation of endocardial and epicardial borders, and the operator adjusted the ROI to best incorporate the entire myocardial thickness **(Figure 1)**. The LV was divided into 7 segments (basal septal, midseptal, apical septal, apical, apical lateral, midlateral, and basal lateral) by the software in accordance with a standard segmentation model used for humans. The operator verified visually that the ROI followed the movements of each segment of the myocardium throughout the cardiac cycle. Retrace of the ROI was attempted if unreliable segments were present, but if these persisted, the dog was excluded from the study. The software algorithm performed speckle tracking across the myocardium, and a weighted average of the myocardial deformation with the weighting greatest at the endocardium was used for strain calculation. Segmental and global strain and SR curves were derived **(Figures 2 and 3)**. The global longitudinal strain waveform was created by the software using a weighted average of the regional strains. Global and segmental peak strain values were automatically provided by the software, while peak systolic and diastolic SR values were offered after placing the cursor at the appropriate time point along the global SR curves.

Event timing for aortic valve closure was recorded from the flow profile of the LV outflow tract obtained by use of pulsed-wave Doppler ultrasonography.

Measurement reliability

To determine intra-observer within-day and between-day measurement variabilities, six echocardiograms were randomly selected from the whole population and subjected to repeated analyses by the same investigator (MJFP) at 2 different time points on a given day and on 2 different days, respectively. Inter-observer measurement variability was also determined as a second investigator (GS) performed independent repeated analyses on the same 6 echocardiograms. The observers were blinded to the results of the previous measurements when performing the analysis.

Statistical analysis

Statistical analysis was performed with commercially available software[c]. Distribution of variables was tested for normality by use of the Shapiro-Wilk test ($\alpha = 0.05$). Data were normally distributed, and mean and standard deviation (SD) for each normally distributed variable were calculated. Further, study population characteristics were analyzed using descriptive statistics and expressed as medians with range.

For the statistical analysis hereunder, as specified for each test, the dogs included were considered as a whole, or were assigned, according to their initial investigations, to one of the two following groups: (1) healthy, or (2) diseased.

To compare the distribution of sex in the healthy versus the diseased group, the chi-squared test was used, while the differences in age or weight were assessed with an unpaired student t-test.

For the repeatability study performed on 6 subjects randomly selected from the whole population, mean and SD values resulting from strain analysis of the repeated examinations were used to determine inter-observer and within-day and between-day intra-observer coefficients of variation (CV), which were quantified as follows: CV = (SD of the measurements/average of measurements) X 100. Further, intra-class correlation coefficients (ICC) for global longitudinal strain values were calculated.

A paired Student *t* test was then used to compare between the 2-D STE variables obtained from the LAp4Ch view and those obtained from the RP4Ch view in the whole population of dogs. To investigate if the sole presence or absence of cardiac disease had an effect on the results obtained, the same test was also performed within the separated groups of healthy and diseased dogs. Limits of agreement were analyzed by Bland-Altman analysis and ICC calculated for global longitudinal strain values, first considering the entire group of dogs and then the separated groups of healthy and diseased dogs.

Values of $P < 0.05$ were considered significant.

Results

Study population

The initial population comprised 87 dogs, but 11 were subsequently excluded due inappropriate tracking of the apical segments throughout the cardiac cycle.

The final study population comprised 76 dogs. Fifty-one dogs were healthy, while 25 had cardiac disease. The healthy group comprised 16 sexually intact females, 15 sexually intact males, 14 spayed females, and 6 castrated males. The age of the dogs in this group ranged from 8 months to 12 years (median, 5.2 years), and the body weight ranged from 12 to 52 kg (median, 28.6 kg). Eight dogs were mixed breeds; all other dogs were purebreds of 17 different breeds, the most common being Boxer (n = 7), Labrador Retriever (n = 7), American Staffordshire Bull Terrier (n = 4) and Doberman Pinscher (n = 4). Five dogs in this group were sedated to aid the echocardiographic examination.

The cardiac disease group comprised patients with a primary diagnosis of myxomatous mitral valve disease (n = 9), coexisting sub-aortic and pulmonic stenosis (n = 3), sub-aortic stenosis (n = 3), tricuspid valve dysplasia (n = 2), idiopathic dilated cardiomyopathy (n = 2), and 1 of each of hypertensive left ventricular hypertrophy, aortic stenosis, mitral valve dysplasia, coexisting pulmonic stenosis and patent foramen ovale, pulmonic stenosis, and right bundle branch block with no identifiable structural heart disease. Nine dogs were sexually intact males, 6 were sexually intact females, 6 were spayed females, and 4 were castrated males. The age of the dogs ranged from 3 months to 15 years (median, 5.9 years), and the body weight ranged from 6 to 48 kg (median, 19.6 kg). Seven dogs were mixed breeds; all other dogs were purebreds of 13 different breeds, the most common being Bull Terrier (n = 2) and Afghan Hound (n = 2). No dog in this group was sedated.

Significant differences were detected comparing healthy and diseased dogs regarding to weight, being healthy dogs heavier (P = 0.000195). No significant differences were present concerning sex or age.

Two-dimensional speckle tracking echocardiography

Eleven out of 87 dogs comprising the initial population had to be excluded from analysis due to inappropriate tracking of the apical segments in the RP4Ch view. Results for 2-D STE variables in the remaining population of 76 dogs were determined **(Table 1)**.

Coefficients of variation were calculated (**Table 2)**. The 6 subjects randomly selected from the whole population for variability analysis included 4 healthy dogs and 2 dogs with cardiac disease (with a diagnosis of myxomatous mitral valve disease and tricuspid valve dysplasia, respectively). The reproducibility of global strain values obtained from the RP4Ch view was very good, as demonstrated by a within-day inter-observer CV of 5,1%, a between-day intra-observer CV of 1,4% and an inter-observer CV of 2,1%. Strain rate values were also within clinically acceptable limits (<15%). For segmental strain indices however, reproducibility was not always good: within-day inter-observer CVs ranged from 8,7% to 19,6%, between-day CV from 1,1% to 14,5%, and inter-observer CVs from 6,5% to 21,7%.

Intra-class correlation coefficients for global longitudinal strain values were also determined as indices of intra- and inter-observer agreement. An excellent degree of congruence (Portney and Watkins, 2009) was found between repeated measurements obtained from the RP4Ch view by the same investigator at different time points on the same day (ICC = 0,968) and on two different days (ICC = 0,989), and between repeated measurements obtained by two different investigators (ICC = 0,987).

Statistically significant differences were found when global and most of segmental strain and SR indices obtained in all dogs from the LAp4Ch view were compared with those obtained from the RP4Ch view **(Table 1)**. More specifically, the absolute values acquired from the RP4Ch view were usually higher. When the analysis was conducted within the separated groups of healthy and diseased dogs, significant differences were still found. However, within the group of healthy dogs, less segmental strain and global SR values showed differences compared with the group of diseased dogs **(Table 1)**. The Bland-Altman scattegrams displaying the differences plotted against average values of the global longitudinal strain values obtained from the LAp4Ch view and the RP4Ch view showed wide limits of agreement, especially within the group of diseased dogs **(Figure 4)**. Besides, the ICC demonstrated only a moderate correlation (Portney and Watkins, 2009) between repeated measurements obtained from the two views in the entire group of dogs (ICC = 0,683), and within the separated groups of healthy (ICC = 0,656) and diseased dogs (ICC = 0,711).

Discussion and conclusions

To the authors' knowledge, the present study was the first in which the use of the RP4Ch view for the assessment of longitudinal strain and SR by use of 2-D STE was investigated in dogs. The results indicated that the above mentioned echocardiographic view can be feasible in healthy and diseased dogs to measure the longitudinal variables mentioned, but careful imaging acquisition and verification is necessary, as tracking errors due to inappropriate visualization of the apical segments during part of the cardiac cycle can occur and invalidate strain data. Further, the values obtained cannot be used interchangeably with those obtained from the most commonly used LAp4Ch view.

In humans, longitudinal deformation is assessed by means of 2-D STE integrating values obtained from the apical two-chamber, four-chamber and five-chamber views (Blessberger and Binder, 2010), and following segmentation models that allow the assignment of individual segments to specific coronary artery territories (Cerqueira et al., 2002). In dogs, only one plane is generally used, and long-axis function of other segments is ignored as regional myocardial dysfunction secondary to myocardial infarcts is less common compared with humans (Wess et al., 2010), and dyssynchrony is not yet routinely assessed for cardiac resynchronization therapy or pacemaker optimization (Estrada and Chetboul, 2006; Gorscan III and Tanaka, 2011, Griffiths et al., 2011). For the scope, the four-chamber view obtained from the left parasternal apical location is typically chosen, and speckle tracking echocardiography performed from this view has been validated against sonomicrometry in an experimental study in dogs (Amundsen et al., 2006). However, breathing artifacts and dropouts can sometimes be present in this projection, especially at the level of the LV free wall and apex, and lower feasibility of 2-D STE measurements obtained in these segments compared to those belonging to the interventricular septum has been reported (Griffiths et al., 2011; Wess et al., 2011).

Different echocardiographic planes might be recommended in the various species based on their peculiar anatomic characteristics (Abduch et al., 2014). For long-axis function assessment by 2-D STE, a subxiphoid approach providing an apical four-chamber view has been chosen in pigs (Ishikawa et al., 2015), left parasternal long-axis planes in mice, rats and rabbits (Kusunose et al., 2012), and sagittal long-axis planes in zebrafish (Hein et al., 2015). In horses, a modified four-chamber view obtained adjusting the standard RP4Ch view is used for longitudinal deformation analysis (Decloedt et al., 2011, 2012). Similarly, the RP4Ch view has been adopted in goats, in which the right parasternal approach is considered the only reliable transthoracic echocardiographic access, as in other ruminants (Abduch et al., 2014; Berli et al., 2015). A good quality four-chamber image can also be attained in most dogs from the right parasternal location (Dukes-McEwan, 2002; Thomas et al., 1993), and the present study demonstrated the ability of 2-D STE to quantify LV longitudinal strain and SR in dogs using this view, with adequate repeatability and reproducibility for clinical use, having most of the measurements CV values <15% (Chetboul et al., 2008). However, it is important to consider that in a relevant proportion of cases (approximately 13% of the initial population), the apical segments were not imaged in their full thickness throughout the whole cardiac cycle, as the epicardial portion ceased to be visible at least partially during diastole. Those cases were consequently excluded from further analysis, as the out of sector motion could limit accurate LV deformation assessment, unless the operator is using a software that bases strain analysis on endocardial tracking, as done in other veterinary studies (Caivano et al., 2016; Carnabuci et al., 2013; Locatelli et al., 2016; Spalla et al., 2016a, 2016b) but not in the current one. In humans and horses, the apical segments are excluded from parasternal derived strain analysis when difficulties acquiring the apical region within the sector arc are present (Decloedt et al., 2011; Forsha et al., 2015), and the same could be necessary in some dogs based on the results of the present study. A more conservative practice would be to discard the measurements if any segments have been excluded.

Intra- and inter-observer variability appeared to be especially good for global longitudinal strain parameters, with CV values always < 10%. However, repeatability and reproducibility were less acceptable for some segmental strain values, with the highest variability observed for the basal septal segment (within-day intra-observer CV 19,6%) and the midlateral segment (inter-observer CV 21,7%). Nevertheless, it should be observed that the LAp4Ch view did not perform superiorly in the present study, as a high variability was also identified assessing some of the same and other segments from this view. Based on these results, 2-D STE would seem less applicable for the assessment of cardiac segmental function in dogs, at least when using the software employed in the present study. Global values are, however, considered an acceptable representation of the entire LV deformation, and are more commonly used than segmental values (Smith et al., 2012; Zois et al., 2012), especially because ischemic cardiomyopathy is not a common disease in dogs. In addition, the segmentation systems used currently by the software employed in the present and in most canine studies could be inaccurate and of little value in dogs, as they are developed to provide the best agreement with the available anatomic data in humans and reflect the coronary perfusion territories, based on clinical application in this species (Cerqueira et al., 2002; Smith et al., 2012; Voigt et al., 2015). Therefore, taking into account that global longitudinal strain could be one of the most commonly used 2-D STE-derived parameter, ICC were also determined in the present study for this specific value, confirming its consistency and reproducibility when obtained from the RP4Ch view.

As imaging the LV from RP4Ch window is often considered technically less demanding, especially in narrow-chested dogs, this view has been previously compared with the left apical one for the evaluation of certain parameters of LV function (Dukes-McEwan, 2002; Wess et al., 2010). In a study involving healthy dogs of different breeds, results of this comparison showed that the RP4Ch view maximized ejection fraction and LV volumes measured with the length-area method, with less marked differences in narrow, deep-chested dogs (Dukes-McEwan, 2002). Another study, including Doberman Pinschers only, determined that LV volume could be measured with the Simpson’s method of discs from either view, with good agreement between both projections (Wess et al., 2010). In the present study, it was demonstrated that the RP4Ch view is not always a viable alternative to the LAp4Ch, as the out of sector motion of the apical segments can invalidate strain data in some dogs. Further, global longitudinal strain and other 2-D STE variables showed significant differences when the two echocardiographic projections were compared, and therefore the measurements obtained are not interchangeable. It is unclear to which extent could the discrepancy observed be related to the presence or absence of cardiac disease, as most of the differences in global and segmental strain values persisted when sub-analysis within the groups of healthy and diseased dogs were performed, while SR values did not show differences in healthy subjects. Further, Bland-Altman analysis provided wider limits of agreement in the group of diseased dogs, while ICC were lower in the group of healthy subjects. Regrettably, the fact that the number of individuals in the two groups was uneven, and that only a few dogs were available for each subcategory of cardiac disease, makes the interpretation of the above results difficult and limits the evaluation of the effects of a specific pathology on the measurements.

As every region in the myocardial walls creates its individual pattern of speckles (Hein et al., 2015), the results obtained could suggest that the two projections image different regions or segments of the LV, even if both display four-chamber planes. For instance, it is reported that the RP4Ch view do not include the true apical region in animals (Abduch et al., 2014). Another explanation could be a difference in the quality of tracking of the segments displayed, related to the distinct orientation of the heart within the plane in the two views. In fact, speckle tracking works better along the ultrasound beam than across beams, and tracking across beams works better in regions adjacent to the transducer than in the far field of the image as lateral resolution decreases in depth with sector probes (Forsha et al., 2015; Støylen, 2013; Voigt et al., 2015). In a study conducted in a human pediatric population, a modest influence of angle insonation and target depth on echocardiographically derived peak systolic longitudinal strain was demonstrated through the comparison of standard windows to alternative ones obtained from near-orthogonal planes, which yielded significant different values (Forsha et al., 2015). The use of echocardiography to obtain the images from which strain is derived would introduce the angle and depth dependence not inherent to strain analysis (Forsha et al., 2015). Axial resolution is superior to lateral resolution, which further worsens in the far field, and image acquisition of the myocardium from different windows can change the ratio of axial to lateral resolution for a given segment (Forsha et al., 2015; Støylen, 2013). The comparison of longitudinal strain values obtained from alternative imaging windows or off-axis apical windows with apically derived strain values derived from standard apical images is therefore discouraged (Forsha et al., 2015), as supported by the results of the present study.

In dogs, a complete echocardiographic examination includes the attainment of the four-chamber view from the left parasternal apical approach, which is essential to analyze the atrioventricular inflows and to perform the TDI analysis, as the Doppler sample volume needs to be aligned parallel to the blood flow and to the myocardial wall, respectively (Abduch et al., 2014; Boon, 2011). Therefore, strain analysis should be performed by 2-D STE on good quality images obtained from this location, as this approach has been validated and more extensively investigated, and values obtained in healthy and diseased dogs are available for comparison (Chetboul et al., 2007, 2008; Hamabe et al., 2015; Santarelli et al., 2017; Smith et al., 2012; Spalla et al., 2016a, 2016b; Suzuki et al., 2013; Takano et al., 2010; Wess et al., 2011; Zois et al., 2012, 2013a, 2013b). However, the use of the RP4Ch view might be considered when the LAp4Ch offers images of suboptimal quality or invalid 2-D STE-derived strain data. In such cases, the view employed for strain assessment should be recorded, and taken into account when results obtained on different occasions from the same individual are compared, as alternating the use of different projections could lead to misinterpretation of any difference as a real change in cardiac function. Further, as previously mentioned, values obtained from the RP4Ch should not be compared with reported values derived from standard apical views.

The present study had limitations. The group of healthy dogs included individuals of several canine breeds with a wide range of weights, and therefore reference ranges were not established. However, it was not the intention of the authors to provide reference ranges, but to assess the feasibility and reliability of the RP4Ch view for longitudinal strain and SR assessment in dogs. Further studies including a larger population of healthy subjects would be needed for the purpose, and separate reference values for different breeds or software may be necessary. In fact, it has been demonstrated that body size impacts long-axis function (Kusunose et al., 2012). Besides, the vendor dependency of the software system used should be taken into account: as the algorithms employed to perform deformation analysis are proprietary, the values obtained in the present study may differ from those obtained by use of another (Voigt et al., 2015). Another limitation for the use of the values obtained in healthy dogs as reference would be the sedation employed in a small number of subjects. Their inclusion in the study was allowed considering the results of a previous study, demonstrating that the sedation protocol used do not affect significantly 2-D STE-derived parameters (Santarelli et al., 2017). Finally, the differences encountered in the comparative study between echocardiographic views may have been complicated by small variations in image quality, cardiac cycles, heart rates, and frame rates there were not statistically evaluated. Regarding heart rate, it did not appear to vary significantly during the scans, and cardiac cycles with stable sinus rhythms were analyzed; further, in a recent study strain and SR variables in the longitudinal direction were not significantly different when various pacing rates were applied (Suzuki et al., 2013c). Besides, by choosing patients with good acoustic windows and image quality, and maintaining frame rates within a narrow range (60–90 Hz), we attempted to minimize these confounders, but we cannot exclude their partial contribution to the differences encountered.

In conclusion, the RP4Ch view was feasible for the assessment of longitudinal strain and SR by use of 2-D STE in healthy and diseased dogs in the present study. However, out of sector motion of the apical segments was present in approximately 13% of the dogs initially included. Further, the deformation parameters obtained were often significantly different from those obtained from the most commonly used LAp4Ch view, and therefore they should not be used interchangeably. Global longitudinal parameters showed a good repeatability and reproducibility, while segmental strains from both views were less reliable, suggesting a safer use of the software system employed for a global assessment of cardiac function in dogs.

Footnotes

a. iE33 ultrasound system, Philips Medical Systems, Andover, Mass.

b. Qlab 2D Strain software, version 9.0, Philips Medical Systems, Andover, Mass.

c. IBM SPSS statistics for Windows, version 19.0, IBM Corp, Armonk, NY.

References

Abduch, M.C., Assad, R.S., Mathias Jr., W., Aiello, V., 2014. The echocardiography in the cardiovascular laboratory: a guide to research with animals. Arq. Bras. Cardiol. 102, 97-103.

Amundsen, B.H., Helle-Valle, T., Edvardsen, T., Torp, H., Crosby, J., Lyseggen, E., Støylen, A., Ihlen, H., Lima, J.A.C., Smiseth, O. A., Slørdahl, S.A., 2006. Noninvasive myocardial strain measurement by speckle tracking echocardiography: validation against sonomicrometry and tagged magnetic resonance imaging. J. Am. Coll. Cardiol. 47, 789-793.

Armstrong, W.F., Ryan, T., 2010a. Evaluation of systolic function of the left ventricle, in: Armstrong, W.F., Ryan, T. (Eds.), Feigenbaum's echocardiography, seventh ed. Lippincott Williams & Wilkins, Philadelphia, pp. 123–157.

Armstrong, W.F., Ryan, T., 2010b. Specialized echocardiographic techniques and methods, in: Armstrong, W.F., Ryan, T. (Eds.), Feigenbaum's echocardiography, seventh ed. Lippincott Williams & Wilkins, Philadelphia, pp. 39-66.

Atkins, C., Bonagura, J., Ettinger, S., Fox, P., Gordon, S., Haggstrom, J., Hamlin, R., Keene, B., Luis-Fuentes, V., Stepien, R., 2009. Guidelines for the diagnosis and treatment of canine chronic valvular heart disease. J. Vet. Intern. Med. 23, 1142-1150.

Berli, A. J., Jud Schefer, R., Steininger, K., Schwarzwald, C.C., 2015. The use of strain, strain rate, and displacement by 2D speckle tracking for assessment of systolic left ventricular function in goats: applicability and influence of general anesthesia. Cardiovasc. Ultrasound 13:11.

Blessberger, H., Binder, T., 2010. NON-invasive imaging: Two-dimensional speckle tracking echocardiography: basic principles. Heart 96, 716-722.

Boon, J., 2011. Veterinary echocardiography, second ed. Blackwell Publishing, Oxford.

Caivano, D., Rishniw, M., Patata, V., Giorgi, M.E., Birettoni, F., Porciello, F., 2016. J. Vet. Cardiol. 18, 146-155.

Carnabuci, C., Hanås, S., Ljungvall, I., Tidholm, A., Bussadori, C., Häggström, J., Höglund, K., 2013. Assessment of cardiac function using global and regional left ventricular endomyocardial and epimyocardial peak systolic strain and strain rate in healthy Labrador retriever dogs. Res. Vet. Sci. 95, 241-248.

Cerqueira, M.D., Weissman, N.J., Dilsizian, V., Jacobs, A.K., Kaul, S., Laskey, W.K., Pennell, D.J., Rumberger, J.A., Ryan, T., Verani, M.S., 2002. Standardized myocardial segmentation and nomenclature for tomographic imaging of the heart: a statement for healthcare professionals from the Cardiac Imaging Committee of the Council on Clinical Cardiology of the American Heart Association. Circulation 105, 539-542.

Chetboul, V., Serres, F., Gouni, V., Tissier, R., Pouchelon, J., 2007. Radial strain and strain rate by two-dimensional speckle tracking echocardiography and the tissue velocity based technique in the dog. J. Vet. Cardiol. 9, 69–81.

Chetboul, V., Serres, F., Gouni, V., Tissier, R., Pouchelon, J.L., 2008. Noninvasive assessment of systolic left ventricular torsion by 2-dimensional speckle tracking imaging in the awake dog: repeatability, reproducibility, and comparison with tissue Doppler imaging variables. J. Vet. Intern. Med. 22, 342-350.

Culwell, N.M., Bonagura, J.D., Schober, K.E., 2011. Comparison of echocardiographic indices of myocardial strain with invasive measurements of left ventricular systolic function in anesthetized healthy dogs. Am. J. Vet. Res. 72, 650–660.

Decloedt, A., Verheyen, T., Sys, S., De Clercq, D., van Loon, G., 2011. Quantification of left ventricular longitudinal strain, strain rate, and displacement in healthy horses by 2-dimensional speckle tracking. J. Vet. Intern. Med. 25, 330-338.

Decloedt, A., Verheyen, T., Sys, S., De Clercq, D., van Loon, G., 2012. Tissue Doppler imaging and 2-dimensional speckle tracking of left ventricular function in horses exposed to lasalocid. J. Vet. Intern. Med. 26, 1209-1216.

Dukes-McEwan, J., 2002. Comparison between right and left cardiac windows to determine left ventricular volumes and ejection fraction in six dog breeds with differing somatotypes. BMUS proceedings. Eur. J. Ultrasound 15, S4-S5.

Estrada, A., Chetboul, V., 2006. Tissue Doppler evaluation of ventricular synchrony. J. Vet. Cardiol. 8, 129-137.

Forsha, D., Risum, N., Rajagopal, S., Dolgner, S., Hornik, C., Barnhart, H., Kisslo, J., Barker, P., 2015. The influence of insonation and target depth on speckle-tracking strain. J. Am. Soc. Echocardiogr. 28, 580–586.

Gorcsan III, J., Tanaka, H., 2011. Echocardiographic assessment of myocardial strain. J. Am. Coll. Cardiol. 58, 1401-1413.

Griffiths, L.G., Fransioli, J.R., Chigerwe, M., 2011. Echocardiographic assessment of interventricular and intraventricular mechanical synchrony in normal dogs. J. Vet. Cardiol. 13, 115-126.

Hamabe, L., Kim, S., Yoshiyuki, R., Fukuyama, T., Nakata, T.M., Fukushima, R., Tanaka, R., 2015. Echocardiographic evaluation of myocardial changes observed after closure of patent ductus arteriosus in dogs. J. Vet. Intern. Med. 29, 126-131.

Hein, S.J., Lehmann, L.H., Kossack, M., Juergensen, L., Fuchs, D., Katus, H.A., Hassel, D., 2015. Advanced echocardiography in adult zebrafish reveals delayed recovery of heart function after myocardial cryoinjury. PLoS One 10: e0122665. Doi:10.1371/journal.pone.0122665.

Ishikawa, K., Aguero, J., Gyun Oh, J., Hammoudi, N., Fish, L.A., Leonardson, L., Picatoste, B., Santos-Gallego, C.G., Fish, K.M., Hajjar, R.J., 2015. Increased stiffness is the major early abnormality in a pig model of severe aortic stenosis and predisposes to congestive heart failure in the absence of systolic dysfunction. J. Am. Heart Assoc. 4:e001925. doi: 10.1161/JAHA.115.001925.

Kusunose, K., Penn, M.S., Zhang, Y., Cheng, Y., Thomas, J.D., Marwick, T.H., Popović, Z., 2012. How similar are the mice to men? Between-species comparison of left ventricular mechanics using strain imaging. PLoS One 7:e40061. doi: 10.1371/journal.pone.0040061.

Lang, R.M., Bierig, M., Devereux, R.B., Flachskampf, F.A., Foster, E., Pellikka, P.A., Picard, M.H., Roman, M.J., Seward, J., Shanewise, J., Solomon, S., Spencer, K.T., St. John Sutton, M., Stewart, W., 2005. Recommendations for chamber quantification: a report from the American Society of Echocardiography's Guidelines and Standards Committee and the Chamber Quantification Writing Group, developed in conjunction with the European Association of Echocardiography, a Branch of the European Society of Cardiology. J. Am. Soc. Echocardiogr. 18, 1440–1463.

Lang, R.M., Badano, L.P., Mor-Avi, V., Afilalo, J., Armstrong, A., Ernande, L., Flachskampf, F.A., Foster, E., Goldstein, S.A., Kuznetsova, T., Lancellotti, P., Muraru, D., Picard., M.H., Rietzschel, E.r., rudski, L., Spencer, K.T., Tsang, W., Voigt, J.U., 2015. Recommendations for cardiac chamber quantification by echocardiography in adults: an update from the American Society of Echocardiography and the European Association of Cardiovascular Imaging. J. Am. Soc. Echocardiogr. 28, 1–39.

Locatelli, C., Spalla, I., Zanaboni A.M., Brambilla, P.G., Bussadori, C., 2016. Assessment of right ventricular function by feature-tracking echocardiography in conscious healthy dogs. Res. Vet. Sci. 105, 103-110.

Portney, L.G., Watkins, M.P., 2009. Foundations of clinical research: applications to practice, third ed. Pearson/Prentice Hall, Upper Saddle River.

Quiñones, M.A., Otto, C.M., Stoddard, M., Waggoner, A., Zoghbi, W.A., 2002. Recommendations for quantification of Doppler echocardiography: a report from the Doppler Quantification Task Force of the Nomenclature and Standards Committee of the American Society of Echocardiography. J. Am. Soc. Echocardiogr. 15, 167–184.

Santarelli, G., Talavera López, J., Fernández del Palacio, J., 2017. Effects of a combination of acepromazine maleate and butorphanol tartrate on conventional and two-dimensional speckle tracking echocardiography in healthy dogs. Am. J. Vet. Res. 78, 158-167.

Silva, A.C., Muzzi, R.A.L., Oberlender, G., Nogueira, R.B., Muzzi, L.A.L., Reis, G.F.M., Mantovani, M.M., 2013. Longitudinal strain and strain rate by two-dimensional speckle tracking in non-sedated healthy cats. Res. Vet. Sci. 95, 1175-1180.

Smith, D.N., Bonagura, J.D., Culwell, N.M., Schober, K.E., 2012. Left ventricular function quantified by myocardial strain imaging in small-breed dogs with chronic mitral regurgitation. J. Vet. Cardiol. 14, 231–242.

Spalla, I., Locatelli, C., Zanaboni, A.M., Brambilla, P., Bussadori, C., 2016a. Echocardiographic assessment of cardiac function by conventional and speckle-tracking echocardiography in dogs with patent ductus arteriosus J. Vet. Intern. Med. 30, 706-713.

Spalla, I., Locatelli, C., Zanaboni, A.M., Brambilla, P., Bussadori, C., 2016b. Speckle-tracking echocardiography in dogs with patent ductus arteriosus: effect of percutaneous closure on cardiac mechanics. J. Vet. Intern. Med. 30, 714-721.

Støylen A. Strain rate imaging: cardiac deformation imaging by ultrasound echocardiography tissue Doppler and speckle tracking, http://folk.ntnu.no/stoylen/strainrate/, 2013.

Sugimoto, K., Fujii, Y., Sunahara, H., Aoki, T., 2015. Assessment of left ventricular longitudinal function in cats with subclinical hypertrophic cardiomyopathy using tissue Doppler imaging and speckle tracking echocardiography. J. Vet. Med. Sci. 77, 1101-1108.

Suzuki, R., Matsumoto, H., Teshima, T., Koyama, H., 2013a. Clinical assessment of systolic myocardial deformations in dogs with chronic mitral valve insufficiency using two-dimensional speckle-tracking echocardiography. J. Vet. Cardiol. 15, 41–49.

Suzuki, R., Matsumoto, H., Teshima, T., Koyama, H., 2013b. Noninvasive clinical assessment of systolic torsional motions by two-dimensional speckle-tracking echocardiography in dogs with myxomatous mitral valve disease. J. Vet. Intern. Med. 27, 69-75.

Suzuki, R., Matsumoto, H., Teshima, T., Koyama, H., 2013c. Influence of heart rate on myocardial function using two-dimensional speckle tracking echocardiography in healthy dogs. J. Vet. Cardiol. 15, 139-146.

Takano, H., Fujii, Y., Ishikawa, R., Aoki, T., Wakao, Y., 2010. Comparison of left ventricular contraction profiles among small, medium, and large dogs by use of two-dimensional speckle-tracking echocardiography. Am. J. Vet. Res. 71, 421-427.

Takano, H., Fujii, Y., Yugeta, N., Takeda, S., Wakao, Y., 2011. Assessment of left ventricular regional function in affected and carrier dogs with Duchenne muscular dystrophy using speckle tracking echocardiography. BMC Cardiovasc. Disord. 11, 23-28.

Thomas, W.P., Gaber, C.E., Jacobs, G.J., Kaplan, P.M., Lombard, C.W., Moise, N.S., Moses, B.L., 1993. Recommendations for standards in transthoracic two-dimensional echocardiography in the dog and cat. Echocardiography Committee of the Specialty of Cardiology, American College of Veterinary Internal Medicine. J. Vet. Intern. Med. 7, 247–252.

Voigt, J., Pedrizzetti, G., Lysyansky, P., Marwick, T.H., Houle, H., Baumann, R., Pedri, S., Ito, Y., Abe, Y., Metz, S., Hyun Song, J., Hamilton, J., Sengupta, P.P., Kolias, T.J., d'Hooge, J., Aurigemma, G.P., Thomas, J.D., Badano, L.P., 2015. Definitions for a common standard for 2D speckle tracking echocardiography: consensus document of the EACVI/ASE/industry Task Force to standardize deformation imaging. Eur. Heart J. Cardiovasc. Imaging 16, 1-11.

Wess, G., Mäurer, J., Simak, J., Hartmann, K., 2010. Use of Simpson's method of disc to detect early echocardiographic changes in Doberman Pinschers with dilated cardiomyopathy. J. Vet. Intern. Med. 24, 1069-1076.

Wess, G., Keller, L.J.M., Klausnitzer, M., Killich, M., Hartmann, K., 2011. Comparison of longitudinal myocardial tissue velocity, strain, and strain rate measured by two-dimensional speckle tracking and by color tissue Doppler imaging in healthy dogs. J. Vet. Cardiol. 13, 31-43.

Zois, N.E., Tidholm, A., Nägga, K.M., Moesgaard, S.G., Rasmussen, C.E., Falk, T., Häggström, J., Pedersen, H.D., Åblad, B., Nilsen, H.Y., Olsen, L.H., 2012. Radial and longitudinal strain and strain rate assessed by speckle-tracking echocardiography in dogs with myxomatous mitral valve disease J. Vet. Intern. Med. 26, 1309–1319.

Zois, N.E., Olsen, N.T., Moesgaard, S.G., Rasmussen, C.E., Falk, T., Häggström, J., Pedersen, H.D., Møller, J.E., Olsen, L.H., 2013. Left ventricular twist and circumferential strain in dogs with myxomatous mitral valve disease. J. Vet. Intern. Med. 27, 875-883.

Figures legend

Figure 1 – Representative 2-D echocardiographic image obtained from a healthy dog providing an end-diastolic right parasternal long-axis view of the LV in which an ROI drawn by the software has been adjusted by the operator manually to better incorporate the entire myocardial thickness. The myocardium has been automatically divided into 7 segments by the software in accordance with standard segmentation models used in humans. The 7 segments are as follows: basal septal (ISB [yellow]), midseptal (ISM [light blue]), apical septal (SApic [green]), apical (Ápice [white]), apical lateral (LApic [purple]), midlateral (ALM [dark blue]), and basal lateral (ALB [red]). Peak strain values for each segment are indicated and represent the corresponding percentage. A simultaneous ECG recording is present. Ick marks on the righ side are at intervals of 5 mm.

Figure 2 - Representative 2-D echocardiographic image obtained from a dog with tricuspid dysplasia (top) and a longitudinal time-strain curve obtained by use of 2-D STE (bottom). In the 2-D image, the myocardium has been divided into 7 segments by the software. The 7 segments are as follows: basal septal (ISB [yellow]), midseptal (ISM [light blue]), apical septal (SApic [green]), apical (Ápice [white]), apical lateral (LApic [purple]), midlateral (ALM [dark blue]), and basal lateral (ALB [red]). Peak strain values for each segment are indicated and represent the corresponding percentage. A simultaneous ECG recording is present. The bottom panel provides color-coded longitudinal strain curves for each segment and a global longitudinal strain curve (dotted white line).

Figure 3 – Representative 2-D echocardiographic image obtained from a healthy dog (top) and a longitudinal time-SR curve obtained by use of 2-D STE (bottom). In the 2-D image, the myocardium has been divided into 7 segments by the software. The 7 segments are as follows:

basal septal (ISB [yellow]), midseptal (ISM [light blue]), apical septal (SApic [green]), apical (Ápice [white]), apical lateral (LApic [purple]), midlateral (ALM [dark blue]), and basal lateral (ALB [red]). A simultaneous ECG recording is present. The bottom panel provides color-coded longitudinal SR curves for each segment and a global longitudinal SR curve (dotted white line).

Figure 4 – Bland-Altman plots for global longitudinal strain (%) in a population of 75 dogs comprising 50 healthy animals and 25 animals with various cardiac diseases (caption A), and within the groups of 50 healthy (caption B) and 25 diseased (caption C) dogs. The differences of the global longitudinal strain values, obtained from the right parasternal four-chamber view and the left apical four-chamber view, are plotted against average values from both views. The mean differences (red middle line) and the range containing the mean of the differences ± 1.96 SD (green lines) are shown.

Table 1—Mean ± SD values for STE-derived longitudinal strain and SR obtained from the LAp4Ch and the RP4Ch views in healthy dogs and dogs with various cardiac diseases.

	Total (n=76)		Healthy group (n=51)		Diseased group (n=25)	
	LAp4Ch	RP4Ch	LAp4Ch	RP4Ch	LAp4Ch	RP4Ch
Global St (%)	–20,6 ±3,8[a]	–23,4 ± 4,4[a]	–20,8 ± 3,2[b]	–23,2 ± 3,3[b]	–20,4 ± 4,9[c]	–23,8 ± 6,1[c]
Basal septal St (%)	–18,6 ±5,6[a]	–20,7 ± 5,5[a]	–18,5 ± 5,7	–20 ± 5	–18,7 ± 5,3[c]	–21,9 ± 6,4[c]
Midseptal St (%)	–24,4 ± 6,7	–24,7 ± 6,3	–24,2 ± 6,4	–25,2 ± 6,4	–23,4 ± 9,1	–28,6 ± 7,9
Apical septal St (%)	–23,8 ±6,7[a]	–27,4± 6,6[a]	–24,1 ± 5,3[b]	–26,9 ± 5,8[b]	–21,8 ± 7,1[c]	–27,7 ± 6,8[c]
Apical St (%)	–22,6 ± 5,4[a]	–26,4 ± 5,7[a]	–22,9 ± 4,3[b]	–25,8 ± 5[b]	–20,6 ± 6,5[c]	–27,4 ± 7,1[c]
Apical lateral St (%)	–21,8 ± 6[a]	–26,1 ± 6,1[a]	–22,4 ± 5,8[b]	–25,4 ± 5,5[b]	–21,8 ± 6,9[c]	–21,8 ± 8,1[c]
Midlateral St (%)	–21 ± 6,4	–22,2 ± 6,4	–20,6 ± 6,1	–22,4 ± 5,5	–21 ± 7,4	–22,4 ± 6,6
Basal lateral St (%)	–21,1 ± 5,9	–22,4 ± 5,7	–21,2 ± 5	–22,4 ± 5,3	–21,2 ± 6,8	–22,5 ± 6,5
Peak S SR (1/s)	-2,3 ± 0,6[a]	-2,5 ± 0,5[a]	-2,4 ± 0,6	-2,5 ± 0,4	-2 ± 0,6[c]	-2,4 ± 0,6[c]
Peak E diastolic SR(1/s)	1,8 ± 0,6[a]	2,3 ± 0,6[a]	1,9 ± 0,5	2,2 ± 0,6	1,7 ± 0,7[c]	2,3 ± 0,7[c]
Peak A diastolic SR(1/s)	1,4 ± 0,6	1,4 ± 0,6	1,4 ± 0,4	1,3 ± 0,6	1,5 ± 0,7	1,5 ± 0,5

[a, b, c] Significant differences between values obtained from the two different views ($P < 0.05$).

St = Strain. S= systolic. SR = Strain rate. E = Early diastolic. A = late diastolic.

Table 2—Intra-observer (within-day and between-day) and inter-observer variability (CV in %) of STE-derived longitudinal strain and SR obtained from the LAp4Ch and RP4Ch views in 6 dogs.

	Intra-observer (Within-day) CV (%)		Intra-observer (Between-day) CV (%)		Inter-observer CV (%)	
	LAp4Ch	RP4Ch	LAp4Ch	RP4Ch	LAp4Ch	RP4Ch
Global St	5,6	5,1	3,1	1,4	3,2	2,1
Basal septal St	16,9	19,6	16,2	6,6	6,6	8,5
Midseptal St	10,4	16,3	20,5	7,1	17,2	12,4
Apical septal St	9,1	9,8	9,6	14,5	17,4	9,7
Apical St	7,3	8,7	6,4	1,1	10	6,5
Apical lateral St	14,1	13,3	9,7	4,8	5,3	7,6
Midlateral St	2,3	17,4	14,1	8,8	14,3	21,7
Basal lateral St	15,6	16,9	10,6	10,2	17,2	16,6
Peak S SR	4,4	9,4	8,1	6,3	7,8	4
Peak E diastolic SR	10,5	10,3	10,8	9,3	8,8	3,6
Peak A diastolic SR	13,6	14,2	11	8,5	14,2	13,1

St = Strain. S= systolic. SR = Strain rate. E = Early diastolic. A = late diastolic.

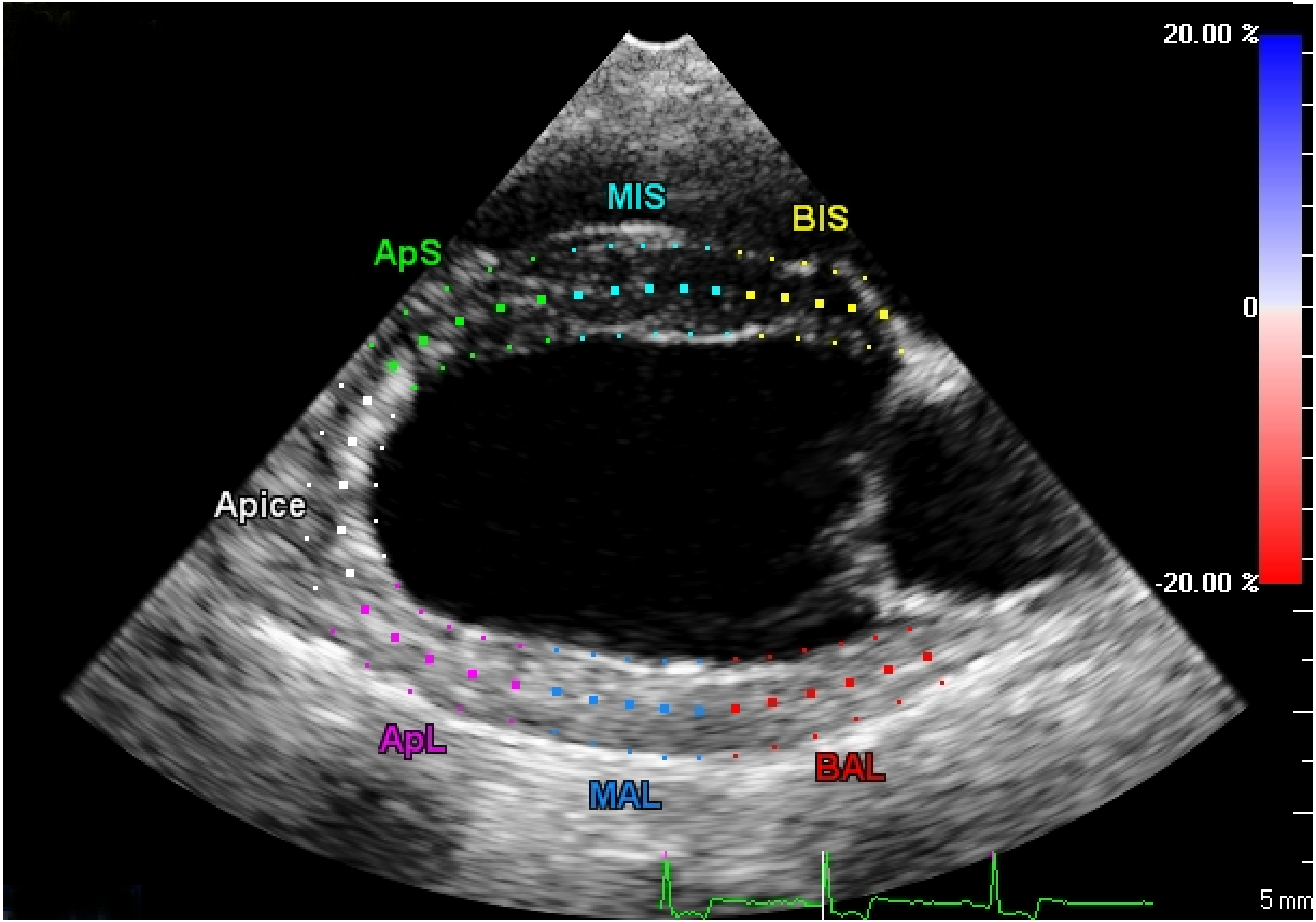

MIS
BIS
ApS
Apice
ApL
MAL
BAL
20.00 %
0
-20.00 %
5 mm

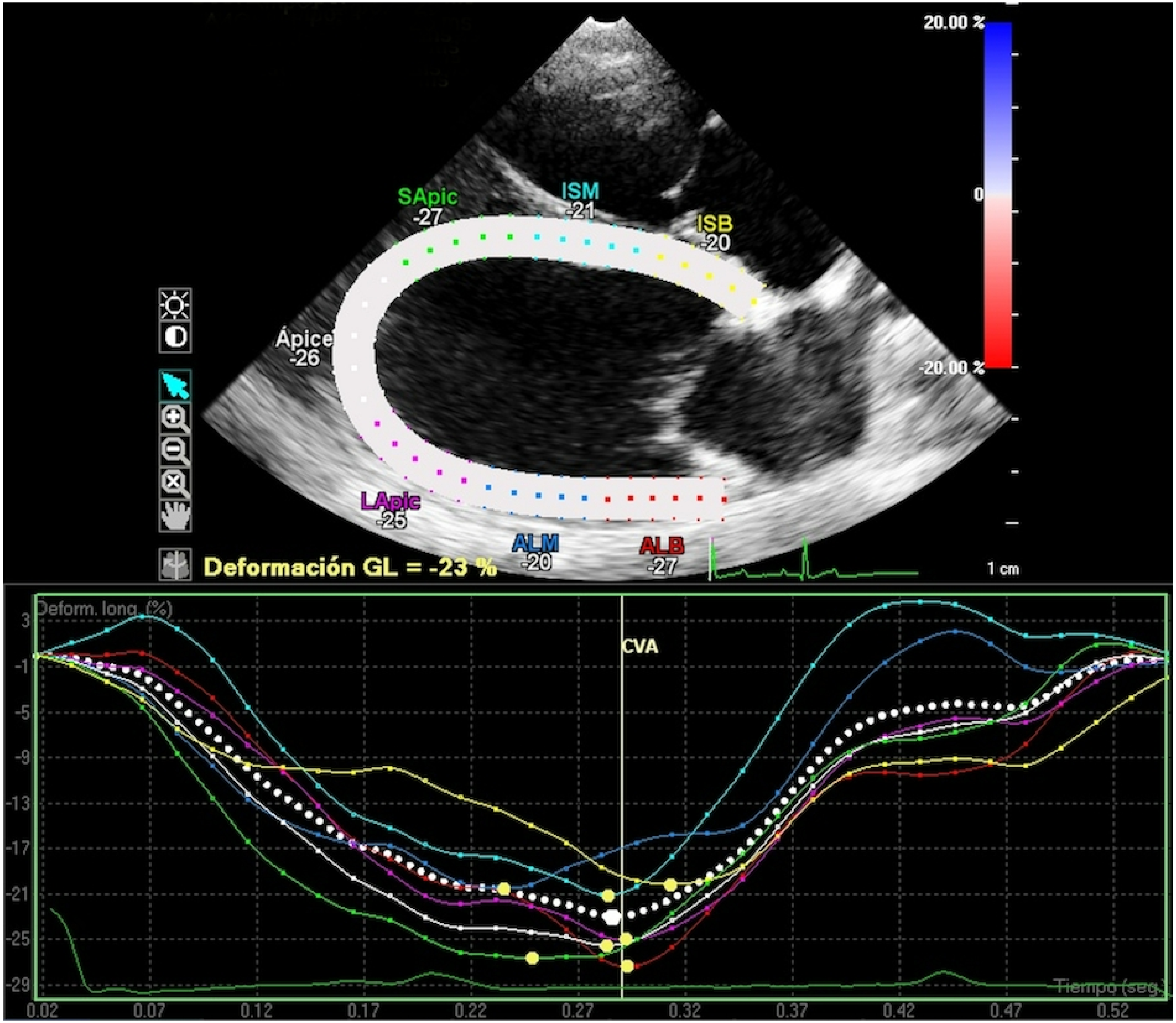

20.00 %
0
-20.00 %
SApic
-27
ISM
-21
ISB
-20
Ápice
-26
LApic
-25
ALM
-20
ALB
-27
1 cm
Deformación GL = -23 %
Deform. long. (%)
CVA
3
-1
-5
-9
-13
-17
-21
-25
-29
Tiempo (seg.)
0.02
0.07
0.12
0.17
0.22
0.27
0.32
0.37
0.42
0.47
0.52

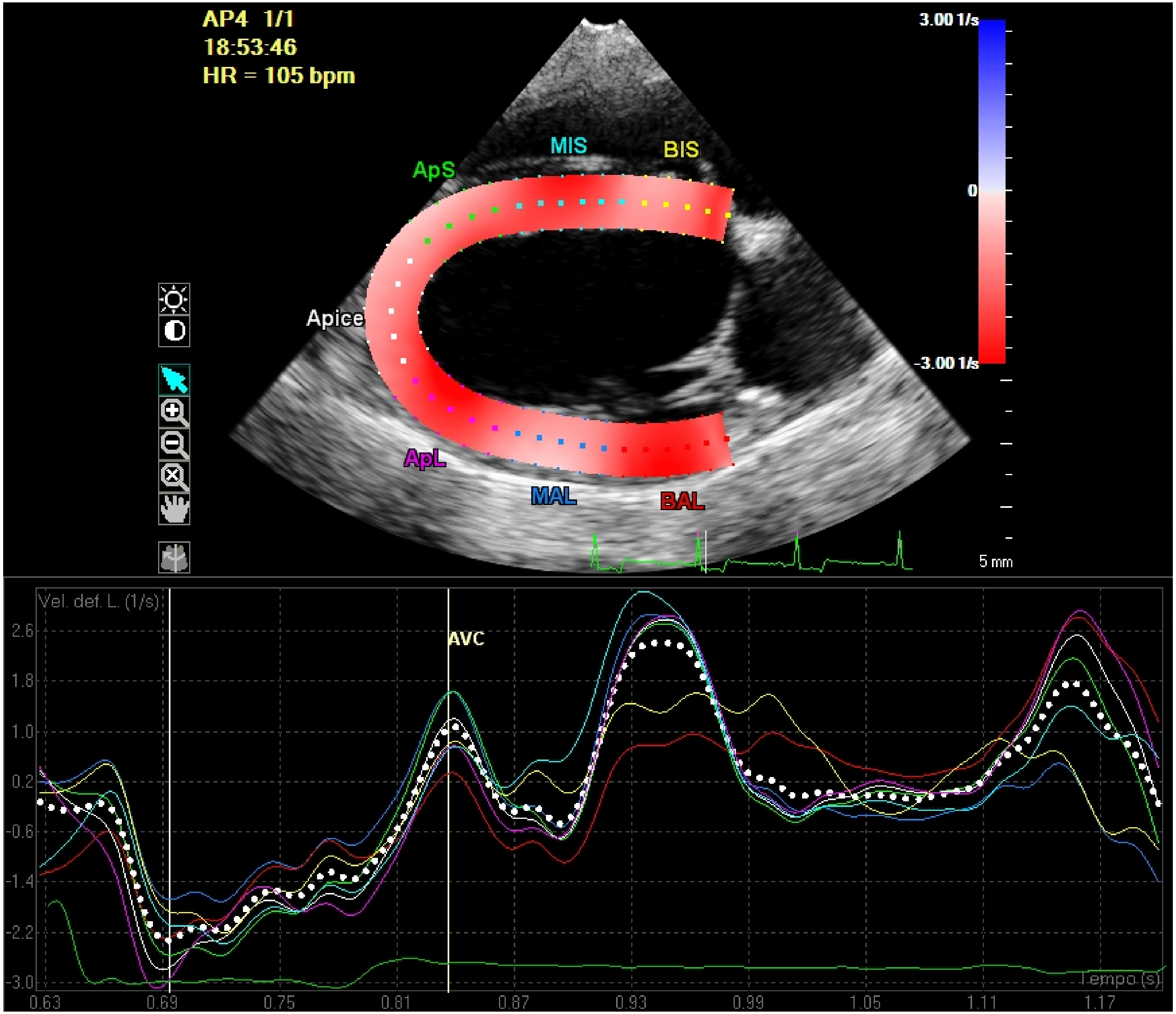
AP4 1/1
18:53:46
HR = 105 bpm
MIS
BIS
ApS
Apice
ApL
MAL
BAL
3.00 1/s
0
-3.00 1/s
5 mm
Vel. def. L. (1/s)
AVC
2.6
1.8
1.0
0.2
-0.6
-1.4
-2.2
-3.0
0.63
0.69
0.75
0.81
0.87
0.93
0.99
1.05
1.11
1.17
Tempo (s)

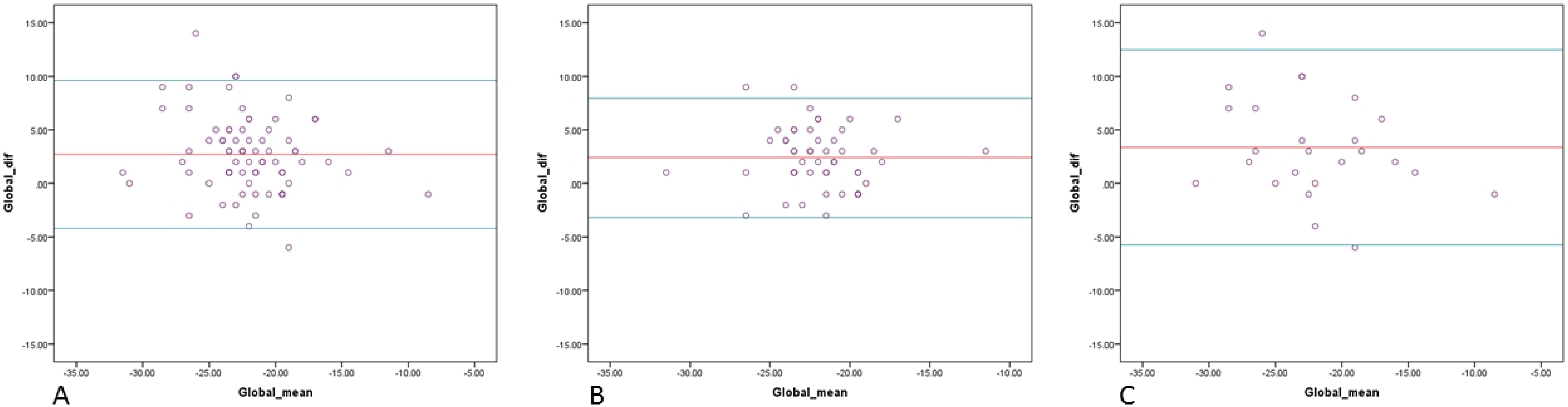
15.00
10.00
5.00
.00
-5.00
-10.00
-15.00
Global_dif
-35.00
-30.00
-25.00
-20.00
-15.00
-10.00
-5.00
Global_mean
A
B
C